Journal of King Saud University – Engineering Sciences (2016) **xxx**, xxx–xxx

King Saud University

Journal of King Saud University – Engineering Sciences

www.ksu.edu.sa
www.sciencedirect.com

ORIGINAL ARTICLES

Adaptive finite element simulation of sheet forming process parameters

Mohd. Ahmed

Civil Engineering Department, Faculty of Engineering, K. K. University, Abha, Saudi Arabia

Received 28 October 2015; accepted 13 October 2016

KEYWORDS

Process parameters;
Adaptive mesh refinement;
Recovery procedures;
Blank and punch radius ratio;
Stretching process;
Drawing process

Abstract The forming processes are influenced by several parameters including dimensions of blank, shape of the tools, mechanical properties of the blank material and type of forming process. In the present study, the sheet metal forming process with varying process parameter is simulated using the adaptive finite element techniques. In an adaptive finite element simulation, the element mesh is automatically refined, coarsened or mesh relocated optimally in areas of insufficient accuracy and sharp strain gradients. A recovery type error estimator based on the energy norm is used for guiding the h-refinement. The simulation results of sheet forming process parameters, namely type of forming process i.e. stretching and drawing, thickness of sheet and, sheet radius and punch radius ratio, are presented and discussed. It is found that the efficiency of process simulation increases with an increase in sheet thickness and decreases with an increase in radius ratios under both stretching and drawing processes.

1. Introduction

The finite element method has won acceptance as a tool for simulation of sheet metal forming operations. Forming operations on thin sheet cause complex deformations in the blank. The nature of deformation in different portions of the blank is generally different. It could range from pure stretching to pure bending, to combined stretching and bending. The recent trend in the simulations is the use of adaptive refined mesh to increase solution accuracy and simulation reliability. The purpose of all adaptive simulations is to obtain numerical solutions efficiently and economically, i.e. restricting the discretization error within permissible limit at minimum computational cost. Sheet forming processes are influenced by several parameters including dimensions of blank, size, and shape of the punch, mechanical properties of the blank material, and radius of the die corner. Tube hydro-forming process was investigated by Jansson et al. (2007) for process parameter estimation such as material feeding and inner pressure considering problem as deformation controlled process. Adaptive mesh free simulation of buckling in sheet metal forming was carried out by Lu et al. (2005). The formability studies of metal in deep drawing process and at elevated temperatures were carried out by Lade et al. (2014) using finite element code LS-DYNA. Kačianauskas et al. (2005) has solved the elastic–plastic problem of SENB specimens using adaptive finite element analysis technique. Adaptive remeshing technique to improve

E-mail address: moahmedkku@gmail.com

Peer review under responsibility of King Saud University.

Production and hosting by Elsevier

http://dx.doi.org/10.1016/j.jksues.2016.10.002

Please cite this article in press as: Ahmed, M. Adaptive finite element simulation of sheet forming process parameters. Journal of King Saud University – Engineering Sciences (2016), http://dx.doi.org/10.1016/j.jksues.2016.10.002

the simulation of metal forming processes utilizing the geometrical and physical error estimators was proposed by Labergere et al. (2008). Energy based adaptive strategy for plates and laminates was presented by Rajagopal and Sivakumar (2009). Solid element adaptive procedures with single and double layer mesh were used by Chung et al. (2014) for simulation of the sheet metal forming process. The adaptive simulation of contact conditions in sheet forming processes was presented by Ahmed et al. (2015). Suresh and Regalla (2014) studied numerical efficiency of the sheet forming process maintaining the same accuracy using shell elements with different element edge lengths and adaptive mesh. An h-type adaptivity using geometric error indicator and based on the mesh free shell formulation was developed by Guo et al. (2013) for the applications in the sheet metal forming simulations. The literature review indicates that research work related to effect of forming process parameters under adaptive environment is scarce. The objectives of the present work is to apply the velocity recovery based adaptive finite element procedures to analyze the effect of parameters, namely, forming process type (stretching and drawing), blank parameters on the deformations during the sheet metal forming process simulation. The adaptively refined mesh zones, i.e. the indicators of the localized deformation zones, and their distributions including the remeshing number required to achieve the predefined accuracy under varying process parameter are studied.

2. Finite element formulation

The basic equations for the finite element model for rigid plastic or rigid visco-plastic material can be derived with the help of the variational principle. It states that among all admissible velocity fields (u_i) that satisfy the conditions of compatibility, incompressibility and the velocity boundary conditions, the actual solution is one that makes the following functional (π) stationary (Oh and Kobayashi, 1980).

$$\pi = \int_V \bar{\sigma}\dot{\bar{\varepsilon}}dV - \int_{S_f} F_i u_i dS \tag{1}$$

where $\bar{\sigma}$, is the effective stress, $\dot{\bar{\varepsilon}}$ is the effective strain rate and F_i represents surface tractions.

In the dual variational problem, the first order variation of the functional vanishes,

$$\therefore \delta\pi = \int_V \bar{\sigma}\delta\dot{\bar{\varepsilon}}\mathrm{dV} - \int_{S_f} F_i \delta u_i \, dS = 0 \tag{2}$$

The incompressibility constraint on the admissible velocity field in Eq. (2) may be incorporated using a penalty term (Zienkiewicz and Taylor, 2000) as given below.

$$\delta\pi = \int_\Omega \bar{\sigma}\delta\dot{\bar{\varepsilon}}d\Omega + k\int_\Omega \varepsilon_v \delta\dot{\varepsilon}_v d\Omega - \int_{\Gamma_f} F_i \delta u_i d\Gamma_f = 0 \tag{3}$$

where k, a so-called penalty constant, is a large positive constant.

Eqs. (2) and (3) may now be discretized in terms of nodal point velocities $\boldsymbol{v}$ of different elements and their variation δV. From arbitrariness of δV_i, the following set of algebraic equations (stiffness equations) are obtained.

$$\frac{\partial\pi}{\partial v_i} = \sum_J \left(\frac{\partial\pi}{\partial v_i}\right)_{(J)} = 0 \tag{4}$$

where J indicates that the quantity referred to pertains to the Jth element. The small-letter suffix signifies that it refers to the nodal point number.

Eq. (4) can be simplified and expressed in the following form.

$$\boldsymbol{K}.\delta\boldsymbol{V} \quad = \boldsymbol{f} \tag{5}$$

where $\boldsymbol{K}$ is called the stiffness matrix and **f** is the residual of the nodal point force vector.

The boundary in metal forming process at time t can be assumed to be divided into three parts, namely S1 on which velocity is prescribed, S2, which is free and S3 where frictional contact occurs. The following conditions apply on each type of boundary.

$$\text{On S1}: \quad (v - vo)\cdot n \quad = 0 \tag{6}$$

$$\text{On S2}: \quad \sigma \cdot n \quad = 0 \tag{7}$$

$$\text{On S3}: \quad \Delta vt \quad = (v - vo)\cdot t \tag{8}$$

where **v**, $\mathbf{v_o}$ are the material and the die velocity, **n** & **t** are unit vectors in the normal and tangential directions with respect to the die surface respectively, and σ is the stress tensor.

The constitutive equation relating deviatoric stresses (σ'_{ij}) and strain rate (ε^*_{ij}) is given as follows,

$$\sigma'_{ij} = 2.\left(\frac{\bar{\sigma}}{3\dot{\bar{\varepsilon}}}\right)\varepsilon^*_{ij} = 2.\mu\varepsilon^*_{ij} \tag{9}$$

The interpolation equations for iso-parametric element can be written as follows.

$$x(\xi,\eta) \quad = N(\xi,\eta)\cdot x \quad \text{and} \quad v(\xi,\eta) = N(\xi,\eta)\cdot v \qquad \dot{\varepsilon} = \boldsymbol{B}\cdot\boldsymbol{v} \tag{10}$$

where ξ, η are the natural coordinates, N is the shape function matrix and B is the strain rate matrix.

The global system equations are obtained from elemental equations through an assembly procedure using the Eq. (4) and (10). A two-point reduced integration is employed for the penalty terms. The non-linear system equation is solved by Newton–Raphson algorithm. To achieve convergence, linear line search technique has been used in the code. A technique based upon the least-squares fitting of velocity field over an element patch has been used to extract derivatives and stresses. An adaptively refined mesh is generated on the basis of the computed error by uniform distribution of the square of error in the elements of the domain until the global error norm is satisfied and predefined solution accuracy is obtained. The energy norm of the error is adopted for assessing of the quality of the solution (Li and Wiberg, 1994) and h-refinement scheme is employed for improving the mesh (Zienkiewicz and Zhu, 1992).

3. Illustrative examples of forming process parameters simulations

A two-dimensional finite element code **AdSheet2**, incorporating the adaptive procedures, was specifically developed for the simulation of sheet forming operation. The validation of the developed code is demonstrated by comparing the predictions of the forming load with those due to Garino and Oliver (1992) and the results of the proposed code is in good

agreement with the literature results. Fig. 2 shows the plots of forming load at different stages of deformation obtained in the present study and those obtained by Garino and Oliver. The code was used to simulate sheet stretching and deep drawing operations by a hemispherical punch. The displacement of punch is applied in incremental steps. Each displacement increment was such that it caused a maximum strain increment of 1%. The adaptive meshes for different process parameters at different stages of deformation, and CPU times required for analyses are studied. The predicted values of effective strain and punch forces for selected process parameters are also discussed. Due to symmetry, only one half of the sheet was modeled. The input parameters adopted were as follows.

Radius of blank, $R_b = 66.0$ mm;
Radius of the die corner $R_d = 6.35$ mm;
Velocity of punch $V = 1$ mm/s;
Blank-holder pressure (drawing) = 5 kN;
Sheet thickness (h) = 1 mm, 2 mm, 3 mm;
Blank to punch radius ratio (R_b/R_p) = 1.33, 1.50, 1.75;
Mesh size reduction factor = 1.2;
Target error = 7%.

$$\text{Stress-strain relation} \quad \bar{\sigma} = 589[0.0001 + \bar{\varepsilon}]^{0.216} \tag{11}$$

where $\bar{\sigma}$ and $\bar{\varepsilon}$ are effective stress and effective strain respectively.

Three cases of sheet thickness namely, 1 mm, 2 mm and 3 mm and three cases of radius ratio of blank to punch namely 1.33, 1.5 and 1.75 were considered for both sheet stretching and drawing process. The radius ratio was taken as 1.33 for studying the sheet thickness analysis. Sheet thickness of 2 mm was used for studying the effect of the radius ratio. The number of elements with uniform mesh in the case of sheet of thickness, 1 mm having two layers of elements, 2 mm and 3 mm having four layers of elements each were 590, 828 and 752 respectively and corresponding degrees of freedom were 2910, 3770 and 3382 respectively for 1 mm, 2 mm and 3 mm sheet thickness (Fig. 1). The accuracy limit was taken as 7% of the global error. Although the analysis provides detailed numerical results for each time increments, the variations in mesh only at a deformation of 20 mm, are studied.

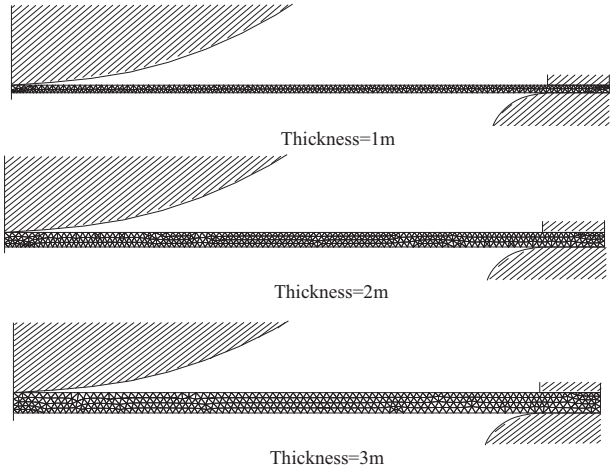

Figure 1 Initial uniform meshes for different thickness (t).

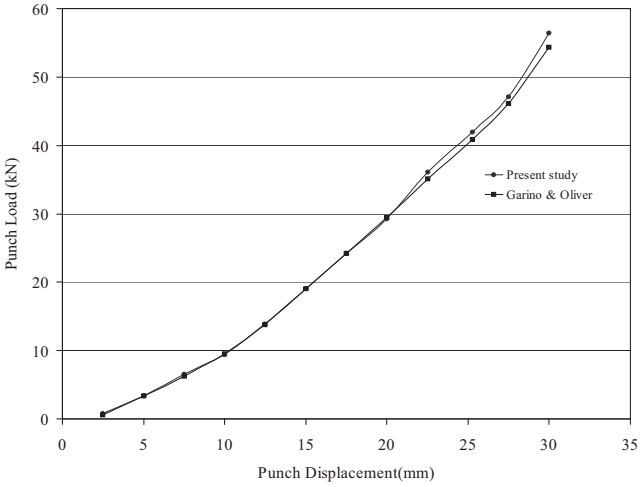

Figure 2 Comparison of load–displacement curves.

3.1. Sheet thickness in stretching and drawing process

The adaptive simulation computational outcomes for different sheet thickness cases of stretching and drawing forming process, with controlled solution error through the total deformation process, are shown in Table 1. Table 1 includes the number of elements in initial mesh, number of mesh regenerations (remeshings) required to get the 7% accuracy, elements in adaptive mesh and total CPU time required for 20 mm deformation. The peak effective strain values and punch load at different stages of deformations with various thicknesses are shown in Table 2. The mesh plots at punch displacement of 20.0 mm for different thickness of sheet for radius ratio of 1.33 are shown in Fig. 3(a) and 3(b) respectively for sheet stretching process and for sheet drawing process.

3.2. Sheet radius to punch radius ratio in stretching and drawing process

The computational results for adaptive simulation of sheet stretching and drawing process having different radius ratios (sheet radius to punch radius) are shown in Table 3. The table depicts initial mesh, number of meshing required to get the 7% accuracy, elements in refined mesh and total CPU time required for 20 mm punch displacement. The adaptive mesh plots at punch displacement of 20.0 mm having blank and punch radius ratios of 1.5 and 1.75 for sheet thickness of 2 mm are shown in Fig. 4(a) and (b) for sheet stretching process and for sheet drawing process. Fig. 3 depicts the adaptive mesh plots of blank and punch radius ratio of 1.33.

4. Discussion

4.1. Sheet thickness

The influence of an important process parameter of sheet forming process namely thickness is studied through adaptive finite element simulation that efficiently captures high stress/strain gradient zones. These zones are the locations of localized deformations. In such zones, mesh is automatically refined, coarsen or mesh relocated in optimal fashion whenever the

Please cite this article in press as: Ahmed, M. Adaptive finite element simulation of sheet forming process parameters. Journal of King Saud University – Engineering Sciences (2016), http://dx.doi.org/10.1016/j.jksues.2016.10.002

Table 1 Adaptive meshing detail and CPU time for stretching and deep drawing process for various sheet thicknesses.

Mesh detail and CPU time	Stretching			Deep drawing		
	h = 1 mm	h = 2 mm	h = 3 mm	h = 1 mm	h = 2 mm	h = 3 mm
Initial mesh elements	590	828	752	590	828	752
No. of remeshings	1	5	2	2	2	4
Adaptive mesh elements	1395	1239 (1st) 1031 (last)	1444 (1st) 1195 (2nd)	2230 (1st) 1200 (2nd)	1443 (1st) 995 (2nd)	1634 (1st) 1602 (last)
Time (h:min)	8:15	7:00	6:30	9:45	4:00	3:00

Table 2 Peak values of effective strain for stretching and deep drawing process for various sheet thicknesses.

Punch displacement (mm)	Stretching			Deep drawing		
	h = 1 mm	h = 2 mm	h = 3 mm	h = 1 mm	h = 2 mm	h = 3 mm
2.5	0.4247	0.4260	0.4476	0.4247	0.4260	0.4476
10.0	0.4928	1.9960	0.5812	0.4495	0.4530	0.4708
15.0	0.6164	2.0010	0.7967	0.4938	0.4931	1.9152
20.0	0.7724	2.0060	1.0732	0.5443	0.5290	2.2348

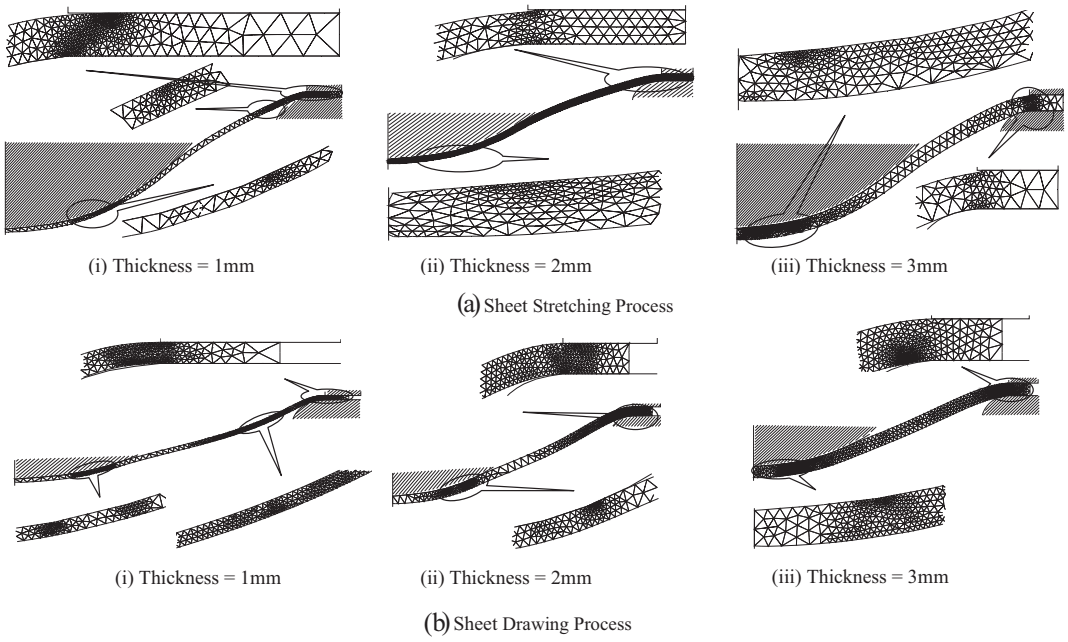

Figure 3 Mesh plots of sheet forming Process for different sheet thicknesses with radius ratio of 1.33 at punch travel of 20 mm.

Table 3 Adaptive meshing detail and CPU time for stretching and deep drawing process for various radius ratios.

Mesh detail and CPU time	Stretching			Deep drawing		
	R_s/R_p = 1.33	R_s/R_p = 1.5	R_s/R_p = 1.75	R_s/R_p = 1.33	R_s/R_p = 1.5	R_s/R_p = 1.75
Initial mesh elements	828	828	828	828	828	828
No. of remeshings	5	1	1	2	1	1
Adaptive mesh elements	1239 (1st) 1031 (2nd)	1480	1432	1443 (1st) 995 (2nd)	1259	1285
Time (h:min)	7:00	12:10	14:15	4	7:15	9:05

Please cite this article in press as: Ahmed, M. Adaptive finite element simulation of sheet forming process parameters. Journal of King Saud University – Engineering Sciences (2016), http://dx.doi.org/10.1016/j.jksues.2016.10.002

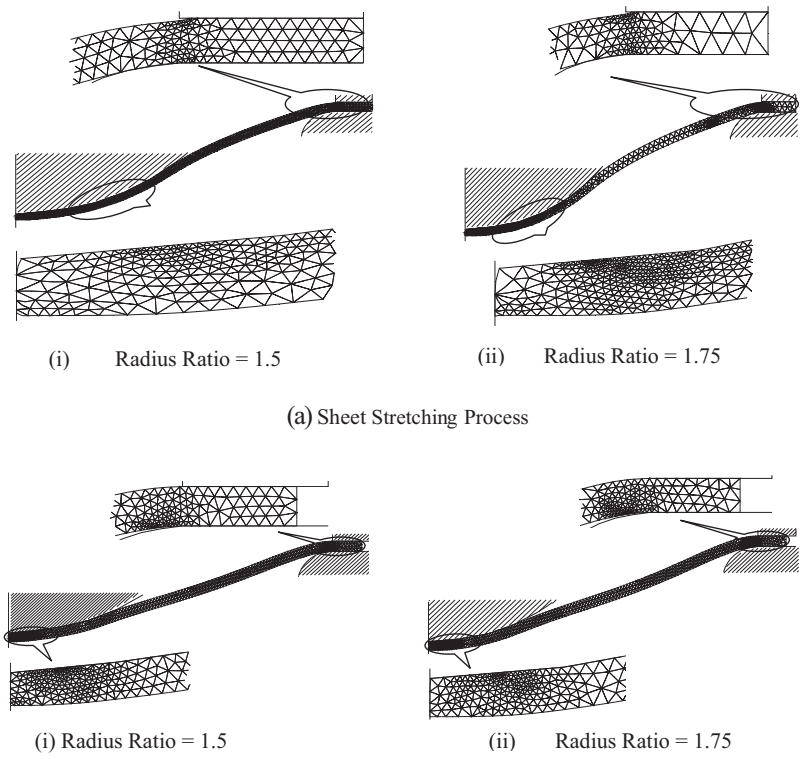

Figure 4 Mesh plots of sheet forming process for different values of radius ratio (R_b/R_P) with thickness of 2 mm at punch travel of 20.0 mm.

error of the solution exceeds the predefined limit of 7%. From the Tabular results and mesh plots of 1 mm, 2 mm and 3 mm sheet thickness under stretching and drawing operation, it is found that an initial uniform mesh becomes adaptively non-uniform and in other word, the locations of localized deformations in sheet forming processes are demarcated. More mesh regenerations are required for a thicker sheet to achieve the target accuracy. In stretching process, five mesh regenerations are required for 2 mm thick while 4 mesh regenerations are needed for 3 mm thick sheets in drawing process. In the first mesh regeneration, the number of elements is increased but with further regeneration, the number of elements is found to decrease in all cases of blank thickness under both stretching and drawing processes. The element density is different in the different portions of the sheet blank. The region of sheet, not in the contact of either punch or die, of various sheet thicknesses has coarser element density as compared to other regions which are in contact with punch or die, during the sheet forming process. With the progress of the forming, the sheet regions in contact with punch or die have zones of finer elements for all sheet thicknesses. The lower sheet thickness has finer elements zone in the non-contacted region also. The finer element zones of contact regions are wider in case of lower thickness of sheet but become narrower with an increase in sheet thickness. It is observed from the adaptive simulation of sheet forming operations with varying blank thickness that the finer element zone moves gradually away from the center of the sheet with an increase in the deformation in both stretching and drawing processes. The distribution of high mesh density zones and their movement describes the localized deformation history during the sheet forming process. The CPU time decreases with the increase in sheet thickness for forming processes studied. The CPU time is more in sheet stretching process than the sheet drawing process for thicker sheet but it is less for lower sheet thickness. It was 9 h 45 min and 8 h 15 min for blank thickness of 1 mm under stretching and drawing operation respectively. Table 2 depicts that the values of peak effective strain for thicker blank are higher as compared to thinner blank for sheet forming processes. The comparison of peak effective strain using the uniform mesh and adaptive mesh given elsewhere (Ahmed and Singh, 2008) indicates that the uniform mesh in simulation suppresses the effective strains. The peak effective strain values for 3 mm thickness of sheet are higher as compared to 1 mm and 2 mm sheet thickness in drawing processes while effective strain values for 3 mm thickness of sheet are higher as compared to 1 mm and lower for 2 mm thickness of sheet in sheet stretching process. For example, the peak values of effective strain at punch displacement of 20.0 mm in sheet stretching process are 0.7724, 2.0060 and 1.0732 respectively for 1 mm, 2 mm and 3 mm thickness of sheet.

4.2. Sheet to punch radius ratio

The role of the radius ratio (ratio of sheet radius to punch radius) during the axi-symmetric stretching and deep drawing process under adaptive environment is examined by varying the radius ratio from 1.33 to 1.75. From the mesh plots of

adaptive results of various radius ratios, it is found that an initial uniform mesh of stretching and drawing process becomes non-uniform after remeshing whenever the error of the solution exceeds the predefined limit and more r mesh regenerations are required for a lower sheet to punch radius ratios. It can also be noted that higher numbers of mesh regenerations are required at a lower radius ratio in sheet stretching process as compared to drawing process. The adaptively generated high density mesh zone is wider under sheet-punch contact region in stretching process simulation while this zone is wider under sheet-die contact region in drawing process simulation. It is also observed that relatively uniform coarse density mesh is generated under non-contacted regions of sheet at lower radius ratio in stretching process, while uniform coarse mesh is generated at higher radius ratio in drawing process under such regions. The CPU time of the sheet stretching and drawing process increases with an increase in radius ratio. The CPU time required for desired deformation is more in sheet stretching process than the time required in sheet drawing process. CPU time was 7 h and 4 h respectively under stretching and drawing process for ratio of sheet radius to punch radius of 1.33.

5. Conclusion

A study of axi-symmetric sheet forming process with important process parameters, namely, forming process type (stretching and deep drawing process), the sheet thickness and radius ratio (defined as the ratio of sheet radius to punch radius) using the adaptive finite element simulation has been carried out. The post-processing type of error estimator has been employed to guide the refinement. The recovery scheme for determining more accurate velocity field is based on the least squares fitting of the computed velocities in elemental patches. Three different cases of sheet thickness and radius ratio for stretching and deep drawing process have been analyzed. The present adaptive finite element simulation study will help to understand the complex deformation process and to reduce the computational cost of high quality simulation of the sheet forming process.

The significant conclusions of the study are summarized below.

1. In the simulation of sheet forming process in adaptive environment, the uniform mesh is automatically refined, coarsened or relocated in optimal fashion whenever the error of the solution exceeds the predefined limit i.e. sheet is divided into coarser and finer mesh zones. The fine mesh zones are the locations of localized deformations. More number of remeshing are required for thicker sheets and for lower ratios of sheet to punch radius to keep the error below the target limit.
2. More number of elements are required to achieve same target accuracy in draw forming process as compared to the stretch forming process. However, distribution of elements i.e. finer or coarser zones is similar in both sheet stretch forming and draw forming processes. Also the number of elements required to reach the predefined error are independent of the initial uniform mesh used for different sheet thickness. The final mesh has more or less same number of elements for various sheet thicknesses.
3. Two zones of high density mesh are observed in sheet forming process for thicker sheets. However, there is more number of such zones for lower values of sheet thickness. The zone of finer elements is located away from the center at lower sheet thickness.
4. The finer element zone moves gradually away from the center of the blank with an increase in deformation in the adaptive simulation of the varying sheet thickness deep drawing process while in the simulation of the varying sheet thicknesses sheet stretching process, no such movement is observed except for lower sheet thickness processing. Also, the finer element zone is wider in the case of lower sheet thickness but becomes narrower with an increase in sheet thickness.
5. Two zones of high density mesh are developed for higher values of radius ratios and more numbers of high density mesh zones are observed for lower radius in the adaptive simulation of sheet stretch forming and draw forming process.
6. The efficiency of process simulation increases with an increase in sheet thickness and decreases with an increase in radius ratios.

References

Ahmed, M., Singh, D., 2008. An adaptive parametric study on mesh refinement during adaptive finite element simulation of sheet forming operations, Turkish. J. Eng. Env. Sci. 32, 163–175.

Ahmed, M., Singh, D., Saiful, I., 2015. Effect of interface contact on adaptive finite element simulation of sheet forming operations. Eur. J. Comput. Mech. http://dx.doi.org/10.1080/17797179.2015.1012632.

Chung, W., Kim, B., Lee, S., Ryu, H., Joun, M., 2014. Finite element simulation of plate or sheet metal forming process using tetrahedron MINI-element. J. Mech. Sci. Technol. 28 (1), 237–243.

Garino, C.G., Oliver, J., 1992. Use of a large strain elastoplastic model for simulation of metal forming process. In: Chenot et al. (Eds.), Numerical Methods in Industrial Forming, pp. 467–472.

Guo, Y., Wu, C.T., Park, C.K., 2013. A meshfree adaptive procedure for shells in the sheet metal forming applications. Interact. Multiscare Mech. 6 (2), 137–156. <http://dx.doi.org/10.12989/imm.2013.6.2.137>.

Jansson, M., Nilsson, L., Simonsson, K., 2007. On process parameter estimation for the tube hydro-forming process. J. Mater. Process. Technol. 190 (1–3), 1–10.

Kačianauskas, R., Stupak, E., Stupak, S., 2005. Application of adaptive finite elements for solving elastic-plastic problem of SENB specimen. Mechanika 51 (1).

Labergere, C., Rassineux, A., Saanouni, K., 2008. Improving numerical simulation of metal forming processes using adaptive remeshing technique. Int. J. Mater. Form. 1, 539–542.

Lade, J., Sasidhar, P.V., Reddy, P.P., Naik, B.B., Gupta, A.K., Singh, S.K., 2014. Formability studies of ASS 304 and evaluation of friction for Al in deep drawing setup at elevated temperatures using LS-DYNA. J. King Saud Univ. Eng. Sci. 26, 21–31.

Li, X.D., Wiberg, N.E., 1994. A posteriori error estimate by element patch post-processing, adaptive analysis in energy and L_2 norms. Compos. Struct. 53 (4), 907–919.

Lu, H., Cheng, H.S., Cao, J., Liu, W.K., 2005. Adaptive enrichment meshfree simulation and experiment on buckling and post-buckling analysis in sheet metal forming. Comput. Methods Appl. Mech. Eng. 194, 2569–2590.

Oh, S.I., Kobayashi, S., 1980. Finite element analysis of plane-strain sheet bending. Int. J. Mech. Sci. 22, 583–594.

Please cite this article in press as: Ahmed, M. Adaptive finite element simulation of sheet forming process parameters. Journal of King Saud University – Engineering Sciences (2016), http://dx.doi.org/10.1016/j.jksues.2016.10.002

Rajagopal, A., Sivakumar, S.M., 2009. Energy based adaptive strategy for plates and laminates. Int. J. Comput. Methods Eng. Sci. Mech. 10 (3), 209–223.

Suresh, K., Regalla, S.P., 2014. Effect of mesh parameters in finite element simulation of single point incremental sheet forming process. Procedia Mater. Sci. 6, 376–382.

Zienkiewicz, O.C., Taylor, R.L., 2000. The Finite Element Method. Butterworth-Heinemann, London.

Zienkiewicz, O.C., Zhu, J.Z., 1992. The super-convergent patch recovery and a posteriori Error estimates. Part I: The error recovery technique. Int. J. Numer. Methods Eng. 33, 1331–1364.

Please cite this article in press as: Ahmed, M. Adaptive finite element simulation of sheet forming process parameters. Journal of King Saud University – Engineering Sciences (2016), http://dx.doi.org/10.1016/j.jksues.2016.10.002